Fibers and Polymers 2013, Vol.14, No.12, 2006-2009 DOI 10.1007/s12221-013-2006-2

Pentacene Crystal Formation on the Surface of Silk Fibroin Films

Youngeun Choi, Young Soo Yun, Se Youn Cho, Min Eui Lee, and Hyoung-Joon Jin*

Department of Polymer Science and Engineering, Inha University, Incheon 402-751, Korea

(Received April 10, 2013; Revised July 1, 2013; Accepted July 9, 2013)

Abstract: Silk fibroin (SF) has attracted interest as a gate dielectric due to its electrical insulation and high mobility in pentacene based organic thin film transistors (OTFTs). In this research, the surface energy of SF is controlled by water annealing, ethanol, and methanol solution treatments in order to study the effect of pentacene morphology on SF thin films with various treatments. For different crystallization methods, the crystal structures and surface energies of SF were investigated in detail by FT-IR and contact angle. Methanol treated SF thin film has a lower surface energy than the other two thin films. Topologies of pentacene on the SF thin films with various surface energies were obtained by atomic force microscopy (AFM). The AFM results showed that the smallest grain size of pentacene was that on methanol treated SF thin film which demonstrated that methanol treated SF thin film can be a proper candidate for a gate dielectric in OTFTs.

Keywords: Silk fibroin, Crystallization, Gate dielectric, Dielectric property, Pentacene

Introduction

Silk fibroin (SF) is a natural fiber that has been used for 3,000 years as one of the most important materials in the textile industry. Especially, SF produced from *Bombyx mori* has been investigated as a potential material for applications in biotechnological and biomedical fields owing to its excellent biocompatible properties and unique mechanical properties [1-4]. Recently, SF has been studied as a suitable platform material for high-technology applications such as photonics and electronics due to its unique characteristics of optical transparency and electrical insulation [5,6]. Above all, SF gate dielectrics have been employed as organic thin film transistors (OTFTs) with high mobility in OTFTs value compared to those fabricated with SiO_2 gate dielectrics [7,8]. This confirms the feasibility of using SF as a gate dielectric in OTFTs.

The surface energy of a gate dielectric has a strong influence on the performance of pentacene thin-film transistors. The surface energy of the gate dielectric greatly affects pentacene deposition conditions, which leads to the changing morphology and microstructure of pentacene, and consequently to changes in charge transport and OTFT performance [9]. It is expected that the surface energy change of a gate dielectric can cause a change in the grain size of the pentacene because the growth mode of the film can be determined by the difference in surface energy between the pentacene and the gate dielectric [10]. Therefore, in order to investigate in detail the effects of the pentacene morphology with respect to the surface energy of the gate dielectric, we controlled the surface energy of the SF gate dielectric.

The surface energy of SF is related to the formation of the highly periodic crystalline regions in the SF. SF serves as an exemplar of fibrous proteins containing crystalline β-sheets. The crystal structure of SF depends on the crystallization method used, such as water annealing, ethanol, and methanol solution treatments [11].

In this study, we controlled the degree of β-sheet structure of SF using water annealing, ethanol and methanol solution treatments. Following the various crystallization methods, the surface energy of the gate dielectrics is controlled by adjusting the crystal structures of SF. We also follow the wettability behavior of the SF thin film surfaces by measuring the contact angle to determine the surface energy characteristics of SF thin films. Also, the morphology of the pentacene deposited on SF thin films was observed for application SF as a gate dielectric.

Experimental

Materials

Cocoons of *B. mori* silkworm silk were purchased by the Ul-jin Sericulture Farm, South Korea. All other materials were purchased from Sigma-Aldrich Co. Ltd.

Preparation of Aqueous SF Solution

The cocoons were boiled for 30 min in an aqueous solution of 0.02 M Na_2CO_3 and rinsed thoroughly with water to extract the glue-like sericin proteins. The extracted silk was then dissolved in a 9.3 M LiBr solution at room temperature to yield a 20 wt% solution. This solution was dialyzed in water using Slide-a-Lyzer dialysis cassettes (Pierce, MWCO 3500) for 36 h. The final concentration of the aqueous silk solution was 7.0-8.0 wt%.

Preparation SF Thin Film and Pentacene Deposition

The SF solution was spin-coated on a silicon wafer. The thickness of the SF thin films was controlled at about 230 nm by adjusting the spin speed. After spin coating, the SF thin films were treated with water, ethanol, and methanol solution for 4 h to induce a crystal structure. After drying, the pentacene was vacuum-deposited (45 nm) on top of the treated SF thin

*Corresponding author: hjjin@inha.ac.kr

films at a base pressure of 5×10^{-6} Torr. The substrate temperature and the deposition rate were 25 °C and 0.1 Å/s, respectively. The SF thin films obtained with different crystallization conditions were named SF_Water, SF_EtOH, and SF_MeOH, corresponding to the treatments of SF.

Characterization

Fourier transform infrared (FT-IR, Bruker, VERTEX 80V, Germany) spectroscopy was used to examine the crystal structure of SF thin films and the thickness of SF thin films was measured by alpha-step (Tencor Ins., Alpha-step 500, USA). The surface energy of SF thin films was evaluated by measuring the contact angles of two test liquids: water and diiodomethane (drop shape analysis system, KRUSS, DSA100, Germany). The dielectric constants at room temperature were measured and calculated by an LCR meter (HP4285A, Hewlett-Packard Co., USA) from 20 Hz to 1 MHz. To observe the roughness of SF thin films and the topology of pentacene on the SF thin films, atomic-force microscopy (AFM, SPA400, Seiko Ins., Japan) was operated in tapping mode.

Results and Discussion

The structure changes in the SF thin films induced by water annealing, ethanol, and methanol solution treatment were confirmed by ATR-FTIR spectroscopy (Figure 1). The amide I (1600-1700 cm^{-1}) and amide II (1450-1600 cm^{-1}) regions were selected to monitor the formation of the β-sheet crystals. The SF thin film initially exhibited a mostly amorphous structure at 1538 cm^{-1} and 1640-1649 cm^{-1} as shown in Figure 1(a). After water annealing, the silk I structure peaks appeared at 1658 cm^{-1} and 1652 cm^{-1} (Figure 1(b)). When the SF film was treated with ethanol, the β-sheet crystal peak appeared, centered at 1626 cm^{-1}. The random coil peaks (1640-1649 cm^{-1}) and the α-helix peak (centered at 1650 cm^{-1}) decreased simultaneously (Figure 1(c)). In Figure 2(d), the SF thin film showed β-sheet vibration bands of amide I (1627 cm^{-1}) and amide II (1514 cm^{-1}) due to the methanol treatment, which is a well-known method for inducing a β-sheet conformation of SF. This change clearly shows the formation of the α-helix and random coil structure from the β-sheet structure (silk II) state [11-13].

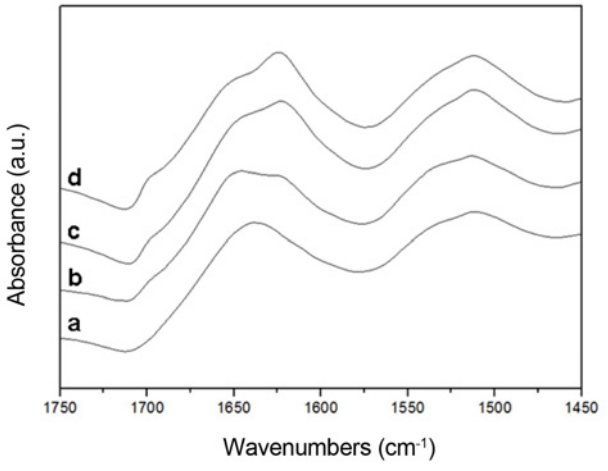

Figure 1. FTIR-ATR spectra of SF thin film (a) no treatment, (b) after water annealing, (c) after ethanol treatment, and (d) after methanol treatment at room temperature for 4 h.

Table 1 shows the dielectric constants (k) of the SF, SF_Water, SF_EtOH, and SF_MeOH. The dielectric constants of SF thin films were about 5.8 at 1 kHz. In a previous work, it was reported that the dielectric constant of SF films prepared by casting on polyethylene dishes was approximately 6 at 3 kHz [14]. These results show that the dielectric constant does not depend on the crystallinity of SF. We also confirmed that SF thin films had a higher dielectric constant than other polymeric materials such as poly(methyl methacrylate) and polyvinyl alcohol [15,16].

The contact angle was measured in order to determine the surface properties resulting from the crystallization. The surface energies of the SF dielectrics after different crystallization treatments are listed in Table 1. These results show that SF_MeOH was found to be more hydrophobic than the water annealed SF thin film. Therefore, we confirmed that the surface energy of SF thin films can be easily controlled as shown in Table 2. Interestingly, degrees of water tension were observed on the surface layers of SF_Water (44.5 °) and SF_EtOH (53.3 °). In contrast, SF_MeOH (63.6 °) showed the highest contact angle among the prepared thin films. This result indicates that treatment for crystallization with SF converts the interfacial property from hydrophilicity to hydrophobicity due to the formation of β-sheet crystal structures. It is also worth noting that the presence of the modified layer yields significantly altered surface free energy on the dielectric, as it is strongly correlated to the grain growth of the surface [17]. Surface energy was calculated from the contact angles with two liquids, di-water and diiodomethane, on each surface using the following equation [18].

Table 1. Dielectric constants of SF, SF_Water, SF_EtOH, and SF_MeOH

	20 Hz	100 Hz	1 kHz	10 kHz	100 kHz	1 MHz
SF	5.9	5.9	5.7	5.5	5.2	3.7
SF_Water	5.9	5.8	5.6	5.4	5.2	5.0
SF_EtOH	6.0	6.1	5.9	5.7	5.4	5.0
SF_MeOH	6.0	6.0	5.8	5.6	5.3	5.1

Table 2. Contact angles and calculated surface energies for the three types of SF thin film surfaces

Contact angle/surface energy	Surface conditions		
	SF_Water	SF_EtOH	SF_MeOH
Contact angle with di-water (°)	44.5	53.3	63.6
Contact angle with CH_2I_2 (°)	36.6	37.2	41.7
Surface energy (mJ/m^2)	55.5	50.3	44.4

$$1+\cos\theta=\frac{2\sqrt{\gamma_s^d\gamma_{lv}^d}}{\gamma_{lv}}+\frac{2\sqrt{\gamma_s^d\gamma_{lv}^d}}{\gamma_{lv}}$$

The surface energy (γ), the dispersion component (γ^d), and the polar component (γ^p) values used to solve this equation were 72.2, 22.0, and 50.2 mJ/m^2 respectively for water, and 50.8, 48.5 and 2.3 mJ/m^2 respectively for diiodomethane.

The roughness of the gate dielectrics is important for the fabrication of OTFTs with good condition of deposited organic semiconductor thin film and device performance [19]. To investigate the influence of roughness on the crystallization, AFM was used to confirm the roughness of crystallized SF thin films. Above all, the surface roughness of gate dielectrics with different surface energies must be similar. Figure 2 shows AFM images of SF_Water, SF_EtOH, and SF_MeOH on heavily doped Si substrates. The surface roughness of the SF thin films is about 0.4 nm thick and has no correlation with crystallization treatments. The surfaces are flat, which is comparable to thermal SiO_2 surface [20].

To confirm the morphology of pentacene on SF thin films, AFM topographies are presented in Figure 3. Figure 3 indicates AFM topographies of nominally one monolayer and 45 nm thick pentacene films on SF_Water, SF_EtOH, and SF_MeOH. The average grain size decreased as the surface energy of gate dielectrics decreased. On the SF_Water with a high surface energy of 55.5 mJ/m^2, pentacene grains exhibited a dendritic structure with larger grains than those of SF_MeOH's.

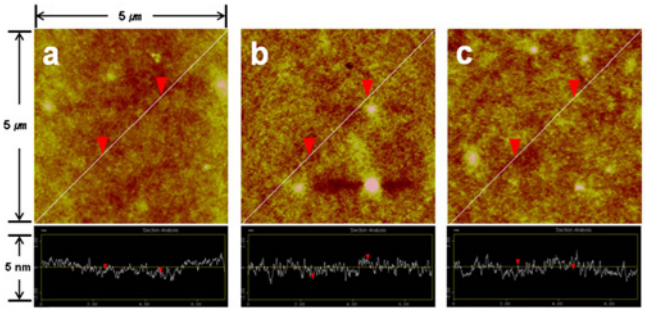

Figure 2. AFM images (5×5 μm) of the surface of SF thin films (a) SF_Water, (b) SF_EtOH, and (c) SF_MeOH (black inset: the depth profile along the white line).

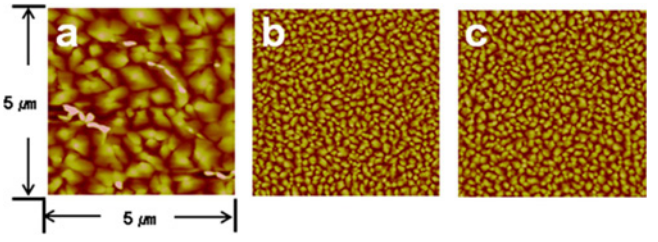

Figure 3. AFM topographies (5×5 μm) of nominally 45 nm thick pentacene films on (a) SF_Water, (b) SF_EtOH, and (c) SF_MeOH gate dielectrics.

However, a drastic morphological change appeared in the pentacene film on SF_MeOH, which has a low surface energy of 44.4 mJ/m^2. Figure 3(c) shows that the pentacene film on SF_MeOH consists of a large number of small grains. The low surface energy of SF_MeOH may help to form an active layer of pentacene with high structural organization and hence smaller crystalline size. This in turn results in efficient charge transport and hence higher carrier mobility.

Conclusion

In this work, we studied the effects of pentacene morphology on SF crystals as a gate dielectric. We successfully controlled the surface energy of SF thin films using water annealing, ethanol, and methanol treatments. Under various treatment methods, dielectric constants and roughness of SF thin films show some similarity. Additionally, we confirmed the influence of pentacene morphology on SF thin films prepared using various methods. To summarize, the pentacene on SF_MeOH is smaller than that on SF_Water. Therefore, it seems that methanol treated SF thin film with efficient charge transport as a gate dielectric is desirable for obtaining high quality pentacene films and for more stable operation of the OTFTs.

Acknowledgment

This study was supported by a grant (#10041220) from the Fundamental R&D Program for Core Technology of Materials funded by the Ministry of Knowledge Economy, Republic of Korea, and by Basic Science Research Program through the National Research Foundation of Korea (NRF) funded by the Ministry of Education (NRF-2013R1A1A2A10008534).

References

1. H.-J. Jin, J. Park, R. Valluzzi, P. Cebe, and D. L. Kaplan, *Biomacromolecules*, **5**, 711 (2004).
2. R. Nazarov, H.-J. Jin, and D. L. Kaplan, *Biomacromolecules*, **5**, 718 (2004).
3. Y. Choi, S. Y. Cho, S. Heo, and H.-J. Jin, *Fiber. Polym.*, **14**, 266 (2013).
4. C. Yumusak and V. Alekberov, *Fiber. Polym.*, **9**, 15 (2008).
5. H. Tao, D. L. Kaplan, and F. G. Omenetto, *Adv. Mater.*, **24**, 2824 (2012).
6. F. G. Omenetto and D. L. Kaplan, *Nat. Photonics*, **2**, 641 (2008).
7. C.-H. Wang, C.-Y. Hsieh, and J.-C. Hwang, *Adv. Mater.*, **23**, 1630 (2011).
8. C.-L. Tasi, L.-S. Tasi, and J.-C. Hwang, *Org. Electron.*, **13**, 3315 (2012).
9. A. Facchetti, C. Kim, and T. J. Marks, *Proc. SPIE.*, 6658 (2007).
10. S. Y. Kwak, C. G. Choi, and B. S. Bae, *Electrochem. Solid State Lett.*, **12**, G37 (2009).

11. H.-J. Jin, J. Park, V. Karageorgious, U.-J. Kim, R. Valluzzi, P. Cebe, and D. L. Kaplan, *Adv. Funct. Mater*., **15**, 1241 (2005).
12. X. Hu, K. Shmelev, L. Sun, E.-S. Gil, S.-H. Park, P. Cebe, and D. L. Kaplan, *Biomacromolecules*, **12**, 1686 (2011).
13. C. Jiang, X. Wang, R. Gunawidjaja, Y.-H. Lin, M. K. Gupta, D. L. Kaplan, R. R. Naik, and V. V. Tsukruk, *Adv. Funct. Mater*., **17**, 2229 (2007).
14. J. Magoshi, *Kobunshi Ronbunshu*, **31**, 456 (1974).
15. J. Puigdollers, C. Voz, A. Orpella, R. Quidant, I. Martın, M. Vetter, and R. Alcubilla, *Org. Electron*., **5**, 67 (2004).
16. J. Veres, S. Ogier, and G. Lloyd, *Chem. Mater*., **16**, 4543 (2004).
17. S. Y. Yang, K. Shin, and C. E. Park, *Adv. Funct. Mater*., **15**, 1806 (2005).
18. J. Kinloch, "Adhesion and Adhesives", Chap. 2, Chapmanand Hall, London, 1987.
19. S. E. Fritz, T. W. Kelley, and C. D. Frisbie, *J. Phys. Chem. B*, **109**, 10574 (2005).
20. C. S. Kim, S. J. Jo, W. J. Lee, H. K. Baik, and S. J. Lee, *Adv. Funct. Mater*., **17**, 958 (2007).